Biorheology 50 (2013) 191–202
DOI 10.3233/BIR-130631
IOS Press

Squeeze film lubrication for non-Newtonian fluids with application to manual medicine

Hans Chaudhry [a], Bruce Bukiet [b,*], Max Roman [a], Antonio Stecco [c] and Thomas Findley [d]

[a] *Department of Biomedical Engineering, New Jersey Institute of Technology, Newark, NJ, USA*
[b] *Department of Mathematical Sciences, New Jersey Institute of Technology, Newark, NJ, USA*
[c] *Department of Physical Medicine and Rehabilitation, University of Padua, Padua, Italy*
[d] *Research Service, VA Medical Center, East Orange, NJ and UMDNJ – New Jersey Medical School, Newark, NJ, USA*

Received 22 October 2012
Accepted in revised form 25 March 2013

Abstract. In this paper, we computed fluid pressure and force on fascia sheets during manual therapy treatments using Squeeze Film Lubrication theory for non-Newtonian fluids. For this purpose, we developed a model valid for three dimensional fluid flow of a non-Newtonian liquid. Previous models considered only one-dimensional flows in two dimensions. We applied this model to compare the one-dimensional flow of HA, considered as a lubricating fluid, around or within the fascia during sliding, vibration, and back-and-forth sliding manipulation treatment techniques. The fluid pressure of HA increases dramatically as fascia is deformed during manual therapies. The fluid force increases more during vertical vibratory manipulation treatment than in constant sliding, and back and forth motion. The variation of fluid pressure/force causes HA to flow near the edges of the fascial area under manipulation in sliding and back and forth motion which may result in greater lubrication. The fluid pressure generated in manual therapy techniques may improve sliding and permit muscles to work more efficiently.

Keywords: Hyaluronic acid, fascia, manual manipulation, massage therapy

AUTHOR COPY

1. Introduction

The goal of this paper is to study fluid flow in three dimensions in biological tissues during massage and related manual therapies. Various massage techniques are used to relieve pain. During these therapies, pressure and tangential force are applied to the skin surface, resulting in deformation of several tissue layers. Most important for our purposes is the layer called the fascia. Fascia is a dense connective tissue that connects muscle, bones and organs, forming a network of tissue throughout the body. It plays an important role in transmitting mechanical forces during changes in human posture to improve postural alignment and other expressions of musculoskeletal dynamics.

There are various types of manual therapies, such as Rolfing (also known as Structural Integration), application of a Massager and Fascial Manipulation. In the Rolfing technique, a compressive and a tangential force are applied simultaneously to the fascia with a constant velocity. In applying a Massager,

* Address for correspondence: Dr. Bruce Bukiet, Department of Mathematical Sciences, New Jersey Institute of Technology, Newark, NJ 07102, USA. Fax: +1 973 596 5591; E-mail: bukiet@njit.edu.

0006-355X/13/$27.50 © 2013 – IOS Press and the authors. All rights reserved

vertical vibrations are applied to the upper layer of the fascia by a mechanical massager with a specified frequency. Fascial manipulation is similar to the Rolfing technique described above except that the therapist provides a back-and-forth oscillation rather than a constant forward sliding velocity. Therapists often claim to increase fascial motion during these therapies resulting in beneficial effects.

Between the fascia and the bone/muscle is a fluid layer of a substance called Hyaluronic Acid (HA). It has been hypothesized that the flow of the HA is important to the benefits of manual medicine. Thus we endeavor to understand the fluid flow of HA fascia during manual medicine.

In [14], we considered HA as a Newtonian fluid. However, there is some controversy as to whether HA acts as a Newtonian or non-Newtonian fluid. Therefore, in this paper, we demonstrate the effects of HA when it is considered as a non-Newtonian fluid. In order to study the behavior of HA as a non-Newtonian fluid, we apply Squeeze Film Lubrication theory for non-Newtonian fluids. We believe that no previous mathematical modeling of the contribution of hyaluronic acid on the upward vertical pressure experienced by the fascia during manual therapy treatments, has been published.

Work in which Squeeze Film theory has been applied to model non-Newtonian fluids has been carried out by Kandasamy and Vishwanath [4,20] to study the behavior in two dimensions for various shapes for Bingham fluids (fluids that include colloidal suspensions, starch paste and lubricating greases). They determined the pressure distribution and load capacity for different values of Bingham numbers and different shapes of squeeze films.

Shukla et al. [15] studied the squeeze film behavior in two dimensions using a power law to express the nonlinear relationship between shear stress and shear strain rate in a fluid. They studied the fluid flow between two parallel plates in cylindrical and spherical geometries and considered both rigid and compliant boundaries. They found that the load capacity increases in layers where the viscosity is high when the boundary is rigid. With compliant boundary layers, the film thickness increases with load.

Sinha et al. [16] also used a power law to model the behavior of a non-Newtonian lubricant fluid between infinitely long rough roller bearings in two dimensions. The model was used to study the case where the rollers are rigid and the case where the rollers are elastic. They found that the effects of the roughness of the bearings are the same whether the lubricant is Newtonian or non-Newtonian. Their model predicts an increase in viscosity in the proximity of a solid surface.

All the above studies were confined to two dimensional analysis in cases where the flow is in one dimension. As far as the authors know, no work has been done to study the behavior of HA. We, therefore, develop equations in this paper that are valid in three dimensions to obtain modified Navier–Stokes equations for non-Newtonian fluids using a non-linear law model for the fluid.

Regarding the presence of HA in connective tissues, Laurent and Fraser [7] reported that Hyaluronan or Hyaluronic Acid (HA) is ubiquitously distributed in the extracellular space of higher animals and that the highest concentrations are found in soft connective tissues. Earlier, Piehl-Aulin et al. [12] observed the presence of HA in human skeletal muscle of lower extremity and that it is abundant in loose connective tissue.

Ellis et al. [1] reported the modified fibroblasts in the inner gliding surface, screening HA. Katzman et al. [5] found an HA-like substance in the inner layer of fresh un-embalmed elderly cadavers.

McCombe et al. [8] found HA concentrated on the inner surface of the deep fascia which is in contact with the underlying muscle. The deep fascia is a multilayered structure of dense and loose connective tissue, which produces a gliding interface in conjunction with the epimysium of the muscle. HA was also found in one of the layers of dense connective tissues [17]. Further, Klein [6] observed HA in the inner gliding layer in the retinaculums of both the ankle and wrist.

AUTHOR COPY

These findings confirm the presence of HA in connective tissues. Tadmor et al. [18] reported the salient characteristics of hyaluronic acid (HA) which he summarized:

1. The role of HA is to assuage compression.
2. HA is not expected to act as a good "boundary lubricant" but it increases the bulk viscosity of synovial fluid that in turn enhances its mode of lubrication.
3. HA is used as a visco-supplementation device and is injected to patients' joints for this purpose.
4. Viscosity of HA decreases considerably with decreasing gap between the two surfaces in which it resides.
5. With loading of the upper surface, the film thickness decreases, while with unloading, the film thickness increases.

We investigated whether the beneficial effects of manual medicine could be due to high pressure generated by HA. It is not unrealistic for thin film layers to experience high pressure. In fact, it has been proposed to use air bearings to support a load of 10^4 kg in airplane engines through use of a 20 micrometer lubricating air layer [10]. For our work, we applied the Squeeze Film theory of fluid mechanics for flow between two plates.

After demonstrating how one can compute the pressure generated in the HA during these therapies, we undertook a comparative study of the flow of HA around or within the fascia in sliding, vertical vibrations and back-and-forth sliding techniques.

AUTHOR COPY

2. Methods

HA is present in the endomysium, perymisium, in the lower layer of fascia and inside the deep fascia. Although HA is in motion in tissues, it is difficult to measure its velocity. Therefore we assume that it is located inside and under the fascia. The film thickness of the HA is around 0.05 mm [17], but it varies from site to site in the body. As observed using ultrasound on the deep fascial layer, when a load is applied on the surface of the skin, the fascial layer below deforms such that a slope is created between the upper and lower fascial layer. The resulting "wedge" that is created in the deformed state is capable of generating pressure within the fluid film when the fluid is subjected to sliding motion. This pressure can lift the upper boundary in much the same way that water between a tire and the road surface can lift a moving car, causing it to lose traction with the road surface (see Fig. 1). The faster the car is moving, the greater the fluid pressure. This model of fascia and HA during manual therapy is consistent with the squeeze film lubrication theory of fluid mechanics.

Since we are considering HA as a non-Newtonian fluid, we need to modify the Navier–Stokes equations valid for Newtonian fluid. To that end, we use a nonlinear law to model the relationship between the shear stress and the shear strain rate, given by, $\tau = B\gamma^n$ where τ is the shear stress and γ is the

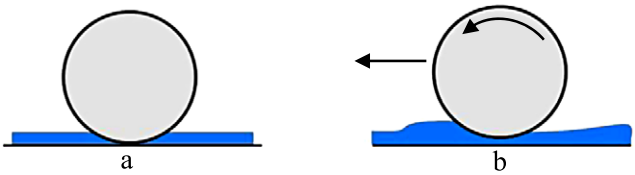

Fig. 1. Thin water film between tire and road surface; (a) stationary: tire and road are in contact; (b) moving: tire and road are separated by the thin film of water. (Colors are visible in the online version of the article; http://dx.doi.org/10.3233/BIR-130631.)

shear strain rate. To evaluate, B and n, we used the experimental shear stress and shear strain data for HA given in [19] and computed the values of B and n that yield the best fit between the theoretical and experimental data. The values of B and n were thus determined to be $B = 0.077$ N s/m^2 and $n = 0.86$ (dimensionless). Using $\gamma = e_{ij} = \frac{1}{2}(\frac{\partial u_i}{\partial x_j} + \frac{\partial u_j}{\partial x_i})$ (as is used in the derivations by Fung [2, p. 375]) where u_i are the velocity components in the Cartesian Coordinates, x_i the stress strain relation becomes:

$$\tau_{ij} = -p\delta_{ij} + Be_{ij}^n, \tag{2.1}$$

where p is the hydrostatic pressure, and δ_{ij} is 1 when $i = j$, and zero, otherwise.

Substituting (2.1) in Euler's equations of motion, the equation of motion for HA modeled as a non-Newtonian fluid reduce to (see the Appendix for details):

$$\begin{aligned}
&\rho\left(\frac{\partial u}{\partial t} + u\frac{\partial u}{\partial x} + v\frac{\partial u}{\partial y} + w\frac{\partial u}{\partial z}\right)\\
&\quad = -\frac{\partial p}{\partial x} + \rho g_x + B\frac{\partial}{\partial x}\left(\frac{\partial u}{\partial x}\right)^n + \frac{B}{2^n}\left[\frac{\partial}{\partial y}\left(\frac{\partial u}{\partial y} + \frac{\partial v}{\partial x}\right)^n + \frac{\partial}{\partial z}\left(\frac{\partial w}{\partial x} + \frac{\partial u}{\partial z}\right)^n\right],\\
&\rho\left(\frac{\partial v}{\partial t} + u\frac{\partial v}{\partial x} + v\frac{\partial v}{\partial y} + w\frac{\partial v}{\partial z}\right)\\
&\quad = -\frac{\partial p}{\partial y} + \rho g_y + B\frac{\partial}{\partial y}\left(\frac{\partial v}{\partial y}\right)^n + \frac{B}{2^n}\left[\frac{\partial}{\partial x}\left(\frac{\partial u}{\partial y} + \frac{\partial v}{\partial x}\right)^n + \frac{\partial}{\partial z}\left(\frac{\partial v}{\partial z} + \frac{\partial w}{\partial y}\right)^n\right],\\
&\rho\left(\frac{\partial w}{\partial t} + u\frac{\partial w}{\partial x} + v\frac{\partial w}{\partial y} + w\frac{\partial w}{\partial z}\right)\\
&\quad = -\frac{\partial p}{\partial z} + \rho g_z + B\frac{\partial}{\partial z}\left(\frac{\partial w}{\partial z}\right)^n + \frac{B}{2^n}\left[\frac{\partial}{\partial x}\left(\frac{\partial w}{\partial x} + \frac{\partial u}{\partial z}\right)^n + \frac{\partial}{\partial y}\left(\frac{\partial v}{\partial z} + \frac{\partial w}{\partial y}\right)^n\right],
\end{aligned} \tag{2.2}$$

where u, v and w are velocities in the x, y and z directions respectively, ρ is the density of the fluid; g_x, g_y, g_z, are the gravitational accelerations along the x, y and z directions. We note that letting $B = 2\mu$ and $n = 1$, Eq. (2.2) reduce to those for the Newtonian case. We also note that since the motion is primarily in the x and z directions, therefore the y momentum equation (the second equation in (2.2)) can be ignored [11].

As HA is incompressible, it must satisfy the continuity equation:

$$\frac{\partial u}{\partial x} + \frac{\partial v}{\partial y} + \frac{\partial w}{\partial z} = 0. \tag{2.3}$$

2.1. Boundary conditions

Referring to Fig. 2, the boundary conditions are as follows:

The lower surface at $y = 0$ is stationary with a velocity $u|_{y=0} = 0$;
The upper surface at $y = h$ moves with velocity $u = U$.
In the z direction, the boundary conditions for the velocity w at $y = 0$ is $w|_{y=0} = 0$
and at the upper surface, $y = h$, the velocity is $w|_{y=h} = 0$. (2.4)

AUTHOR COPY

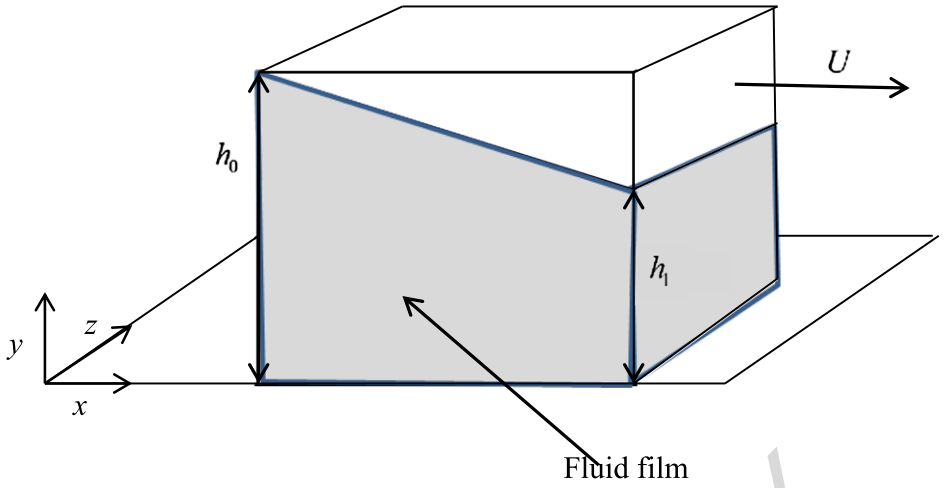

Fig. 2. Squeeze film model of rolfing. In rolfing, the manual manipulation is steady and in one direction. For Fascial Manipulation the motion is back and forth with sinusoidal velocity. (Colors are visible in the online version of the article; http://dx.doi.org/10.3233/BIR-130631.)

AUTHOR COPY

The pressure along the edges is assumed to be $p = 0$, i.e., gauge pressure.

As the film is very thin compared to the length and width of the fascia being considered (see Fig. 2), we perform the following scaling, see [11]:

$$x, z \approx L; \qquad y \approx h; \qquad u, w \approx U; \qquad v \approx \frac{Uh}{L}, \tag{2.5}$$

where h is the film thickness. Since the flow is primarily in the x and z directions, the y-momentum equation in (2.2) may be neglected. Then, applying the scaling (2.5) in the remaining two equations of (2.2), these equations become:

$$\begin{aligned} \frac{\partial p}{\partial x} &= \frac{Bn}{2^n}\left[\left(\frac{\partial u}{\partial y}\right)^{n-1}\frac{\partial^2 u}{\partial y^2}\right], \\ \frac{\partial p}{\partial z} &= \frac{Bn}{2^n}\left[\left(\frac{\partial w}{\partial y}\right)^{n-1}\frac{\partial^2 w}{\partial y^2}\right]. \end{aligned} \tag{2.6}$$

Integrating these equations, subject to boundary conditions in (2.3) yield expressions for the velocity components, u and w:

$$\begin{aligned} u &= U\frac{y}{h} + \frac{2}{B^{1/n}}\frac{\partial p}{\partial x}\left[\frac{y^{(n+1)/n}}{(n+1)/n} - y\frac{h^{1/n}}{(n+1)/n}\right], \\ w &= \frac{2}{B^{1/n}}\frac{\partial p}{\partial z}\left[\frac{y^{(n+1)/n}}{(n+1)/n} - y\frac{h^{1/n}}{(n+1)/n}\right]. \end{aligned} \tag{2.7}$$

Using (2.7) in the continuity Eq. (2.3), we get, after some simplifications, the following equation for determining the pressure p

$$\frac{\partial}{\partial x}\left[h^{(2n+1)/n}\left(2-n^2\right)\frac{\partial p}{\partial x}\right]+\frac{\partial}{\partial z}\left[h^{(2n+1)/n}\left(2-n^2\right)\frac{\partial p}{\partial z}\right] = B^{1/n}(n+1)(n+2)\left[\frac{U}{2}\frac{\partial h}{\partial x}+\frac{\partial h}{\partial t}\right]. \tag{2.8}$$

We note that letting $B = 2\mu$ and $n = 1$, Eq. (2.8) agrees with the Newtonian case [11]. Here h is a function of x and $\frac{\partial h}{\partial t}$ represents the vertical velocity. From Fig. 2, $h(x)$ is given by:

$$h(x) = h_0 - (h_0 - h_1)\frac{x}{L}. \tag{2.9}$$

For an infinitely wide bearing, the flow can be assumed to be uni-directional [3,4,12,15,16]. In our case the length L (approximated as 0.025 m) (Fig. 2) is very large compared to the film thickness of about 0.05 mm [17]. Thus, Eq. (2.8) for one-dimensional flow reduces to

$$\frac{\mathrm{d}}{\mathrm{d}x}\left[h^{(2n+1)/n}\left(2-n^2\right)\frac{\mathrm{d}p}{\mathrm{d}x}\right] = B^{1/n}(n+1)(n+2)\left[\frac{\mathrm{d}h}{\mathrm{d}x}\left(\frac{U}{2}\right)+\frac{\partial h}{\partial t}\right]. \tag{2.10}$$

3. Results

3.1. *Case* 1: *Rolfing or sliding*

In this technique, a tangential force with a constant horizontal velocity U is applied on the upper surface of the fascia. Therefore, in (2.10), the vertical velocity $\frac{\partial h}{\partial t}$ is ignored.

Then, using (2.9) in (2.10) with the condition that $p = 0$ at $x = 0$ and at $x = L$, the pressure, p, is given by

$$p(x) = \frac{\beta U n}{\alpha(2-n^2)}\left[\left\{(h_0-\alpha x)^{-1/n} - (h_0)^{-1/n}\right\} - \frac{h(m_1)}{n+1}\left\{(h_0-\alpha x)^{-(n+1)/n} - (h_0)^{-(n+1)/n}\right\}\right], \tag{3.1}$$

where

$$\beta = \frac{B^{1/n}(n+1)(n+2)}{2}; \qquad \alpha = \frac{h_0-h_1}{L}; \qquad h(m_1) = \frac{(n+1)[(h_1)^{-1/n} - (h_0)^{-1/n}]}{[(h_1)^{-(n+1)/n} - (h_0)^{-(n+1)/n}]}.$$

The parameters used in the above are: $B = 0.077$ N s/m^2, $n = 0.86$, $h_0 = 50$ μm, $h_1 = 40$ μm, $L = 25$ mm and $U = 0.1$ m/s.

Using these parameters, the vertical fluid force on the fascia sheet is shown in Fig. 3.

AUTHOR COPY

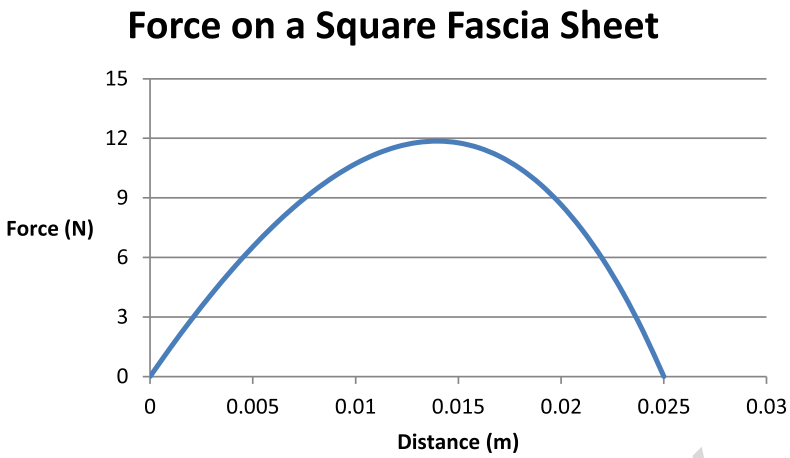

Fig. 3. The vertical fluid force on a square sheet of fascia varying along the length of fascia using the parameters given in the text for the case of constant tangential velocity using the rolfing technique (Case 1). (Colors are visible in the online version of the article; http://dx.doi.org/10.3233/BIR-130631.)

In all the cases studied, the total vertical fluid force, F on the square sheet of fascia is given by the expression

$$F = L \int_0^L p(x)\,\mathrm{d}x.$$

3.2. *Case* 2: *Massager* (*vertical vibrations*)

In the case of vibration there is no slope component (i.e., $h_0 = h_1$), as can be seen from Eq. (2.10). Only the change in height due to the vibratory motion is important. In this case we use a film whose thickness varies only in the vertical direction. Again a film thickness of 50 μm was used with a frequency of 15 Hz, with maximum amplitude, A equal to 10 μm. We consider the height to obey the equation $h(t) = A\sin^2(\omega t)$.

Thus, the solution of (2.10) with the same boundary conditions as in case 1, results in:

$$p(x,t) = \beta\left(\frac{x^2}{2} - \frac{xL}{2}\right)h_0^{-(2n+1)/n}, \tag{3.2}$$

where

$$\beta = \frac{B^{1/n}(n+1)(n+2)}{2-n^2}A\omega\sin(2\omega t).$$

The fluid force plot is shown in Fig. 4 for $h(0) = 50$ μm.

3.3. *Case* 3. *Fascial manipulation* (*back and forth motion*)

The case of Fascial Manipulation is similar to the Rolfing technique described above, except that the therapist provides back and forth oscillations, $U(t)$, rather than a constant velocity. Equation (2.10) then

AUTHOR COPY

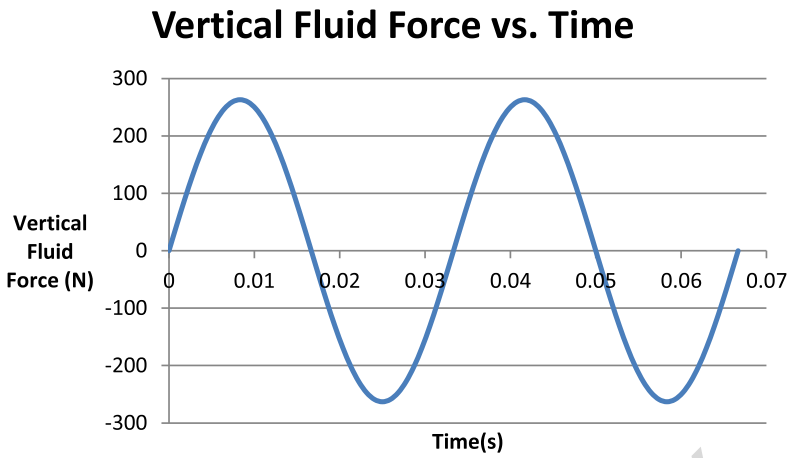

Fig. 4. The vertical fluid force on a square sheet of fascia varying in time at the midpoint of the fascia using the parameters given in the text for the case of vertical vibration (massage; Case 2). The results presented are for a frequency of 15 Hz. (Colors are visible in the online version of the article; http://dx.doi.org/10.3233/BIR-130631.)

becomes

$$\frac{\mathrm{d}}{\mathrm{d}x}\left[h^{(2n+1)/n}\left(2-n^2\right)\frac{\mathrm{d}p}{\mathrm{d}x}\right] = B^{1/n}(n+1)(n+2)\left[\frac{\mathrm{d}h}{\mathrm{d}x}\left(\frac{U}{2}\right)\right]. \tag{3.3}$$

Here $U(t)$ is taken as $U(t) = d\sin(\omega t)$, where d is the maximum displacement which is taken to be 0.1 m and the frequency of oscillations is taken as 2 Hz. Solving (3.3) under the boundary conditions, $p = 0$ at $x = 0$ and at $x = L$, the pressure $p(x,t)$ is given by:

$$p(x,t) = \frac{\beta_1 n}{\alpha(2-n^2)}\left[(h_0-\alpha x)^{-1/n} - h_0^{-1/n}\right] - \frac{\gamma(nx)}{(2n+1)(2-n^2)} + \frac{\delta n}{(2-n^2)(n+1)\alpha}\left[(h_0-\alpha x)^{-(n+1)/n} - h_0^{-(n+1)/n}\right], \tag{3.4}$$

where

$$\beta_1 = \frac{B^{1/n}(n+1)(n+2)}{2}U(t), \qquad \gamma = \rho(2n+1)(2-n)\frac{\mathrm{d}U}{\mathrm{d}t}.$$

And δ can be found from:

$$\frac{n\delta}{(2-n^2)(n+1)\alpha}\left[h_1^{-(n+1)/n} - h_0^{-(n+1)/n}\right] = \frac{\gamma n L}{(2n+1)(2-n^2)} - \frac{\beta_1 n}{\alpha(2-n^2)}\left(h_1^{-1/n} - h_0^{-1/n}\right). \tag{3.5}$$

Here ρ is the density and is equal to 3.4 gm/l. The fluid force plot is shown in Fig. 5.

AUTHOR COPY

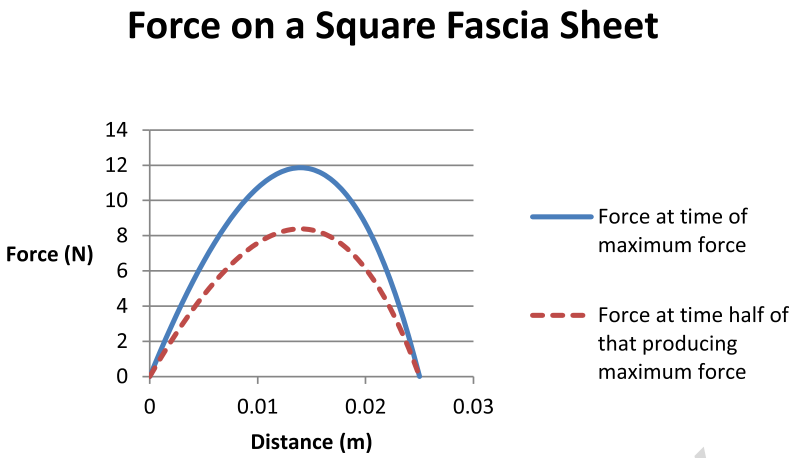

Fig. 5. The vertical fluid force on a square sheet of fascia varying along the length of fascia using the parameters given in the text for the case of back and forth motion (fascial manipulation; Case 3). Results are given at the time of maximum force and at half that time. The case shown is for frequency of 2 Hz. The force is approximately linearly proportional to the frequency. (Colors are visible in the online version of the article; http://dx.doi.org/10.3233/BIR-130631.)

4. Discussion

From Eqs (3.1) and (3.3) it can be seen that a non-zero slope is necessary to generate a fluid pressure during sliding manipulation. That is, there must be a difference in film thickness between the right and left edges. If the film thickness is constant throughout, there will be no fluid pressure generated. It has been seen using ultrasound imaging that there is indeed a variation in deformation throughout the fascia when a load is applied on the surface of the skin. We use the film thickness of 50 μm [17] with a variation of 10 μm between the right and left edge for both the sliding and back-and-forth manipulation.

The velocity used in our study of sliding motion (case 1) is a constant 0.1 m/s. This value was obtained by observing manual therapy in using the Rolfing technique. Typical hand held massagers operate at a low end frequency of 15 Hz and high end frequency of 60 Hz. We present results in case 2 for a frequency of 15 Hz. For the back-and-forth sliding (case 3) frequencies of 2 and 4 Hz have been used, which are practical estimates of the oscillatory frequency achievable in manual therapy.

The comparative study results of the fluid force on the fascia sheet generated by HA with each therapy and for the Newtonian and non-Newtonian cases are presented in Table 1. As can be seen, sliding therapy and fascial manipulation (back-and-forth) results in much lower fluid force generated on the fascia sheet. While the fluid force is highly dependent on the velocity at which the therapy is applied, with higher velocities generating a greater fluid pressure, in practice velocities greater than 0.1 m/s are not generally applied. As the frequency of the motion increases the fluid force increases linearly. Finally, it can be seen that the vertical vibrations (massager) result in the highest fluid forces. At 15 Hz, the fluid force is many times greater than the sliding and back-and-forth motion. Again, this is due to the greater velocities that can be used in applying vibration versus sliding. However, it should be noted that while greater fluid forces are generated during oscillatory motion such as vibration and back-and-forth sliding, the force increases and decreases during the administration of the treatment. In sliding motion, the fluid force is lower, but it is maintained at the same level throughout the sliding motion. Each therapy may have its own advantages. The effects should be looked at in greater detail in further studies.

AUTHOR COPY

Table 1
Comparative study of Rolfing, Vertical Massage and Fascial Manipulation (back-and-forth motion)

Method	Total force (N)		
		Non-Newtonian	Newtonian
Rolfing		7.85	3.32
Vertical massage (frequency 15)		167	74
Back-and-forth sliding	5.0	Frequency = 2; Max velocity = 0.1 m/s	2.1
	10.0	Frequency = 4; Max velocity = 0.2 m/s	4.2

Notes: Total force on the fascia sheet for each case is presented. Total force is given by the average force multiplied by the area of the fascia sheet.

5. Conclusions

The fluid pressure of HA increases dramatically as fascia is deformed during manual therapies. For a 10 μm decrease in the fascial layer thickness at the two edges, the magnitude of the fluid force on a square fascia sheet of 25 × 25 mm in the Rolfing technique is on the order of 8 N. It has also been seen that there is a greater increase in force during vibratory manipulation treatment compared to constant sliding, and that the maximum force is highly dependent on the frequency of vibration. It has also been observed that there is a negative fluid force (due to suction) during vibratory treatment. The variation of pressure in constant sliding and back and forth motion will cause HA to flow towards the edges of the fascial area under manipulation whereas in vertical vibratory treatment the flow will alternate between the center and the edges. These flows may result in greater lubrication. Another implication of the mathematical findings is that they provide an explanation of the decrease in adhesion between different tissues that therapists feel during Rolfing and during back and forth treatment. Patients' reports confirm this phenomenon. It is not clear whether any change in lubrication continues after manipulation ceases. Therefore subsequent sessions may be required to continue lubrication unless other longer lasting structural changes are taking place, perhaps similar to the connective tissue structures which allow tendon sliding noted in [3]. The fluid pressure generated in rolfing and back-and-forth motion between the two layers (fascia and bone) causes the fluid gap to increase, and consequently the thickness between the two layers to increase. The presence of a thicker fluid gap can improve the sliding system and permit the muscles to work more efficiently. While the recent developments in musculoskeletal ultrasound can image fluid layers of 100–200 microns, anatomical investigations at even higher resolution will be needed to evaluate structural connective tissue changes, using sheet plastination [9] or second harmonic imaging [13]. Also actual measurements of loading and shear forces during manual therapy may lead to more accurate modeling. Our studies show that with an increase in slope between the two edges, the fluid force increases non- linearly. Again the fluid force is observed to be higher for HA modeled as non-Newtonian HA than for HA modeled as a Newtonian fluid.

AUTHOR COPY

Acknowledgements

The authors wish to acknowledge the helpfulness of the referees and the editor whose efforts have greatly improved this paper. This work was funded in part by a grant from May-Hill Medical Group of New Jersey.

Appendix

To derive Eq. (2.2) from Eq. (2.1) we follow the strategy as given in Fung [2].
Euler's equation of motion is given by

$$\rho\frac{Dv_i}{Dt} = \frac{\partial\tau_{ij}}{\partial x_j} + X_i, \tag{A1}$$

where ρ is the density, X_i is the body force component $(\rho g_x, \rho g_y, \rho g_z)$ and v_i are velocity components (u, v, w) and $\frac{D}{Dt} = (\frac{\partial}{\partial t} + u\frac{\partial}{\partial x} + v\frac{\partial}{\partial y} + w\frac{\partial}{\partial z})$. Using Eq. (2.1), we arrive at

$$\begin{aligned}
\tau_{11} &= -p + B(e_{11})^n = -p + B\left(\frac{\partial u}{\partial x}\right)^n,\\
\tau_{12} &= B(e_{12})^n = \frac{B}{2^n}\left(\frac{\partial u}{\partial y} + \frac{\partial v}{\partial x}\right)^n,\\
\tau_{13} &= B(e_{13})^n = \frac{B}{2^n}\left(\frac{\partial u}{\partial z} + \frac{\partial w}{\partial x}\right)^n.
\end{aligned} \tag{A2}$$

Using Eq. (A2) in the first of Eq. (A1) we obtain:

$$\begin{aligned}
&\rho\left(\frac{\partial u}{\partial t} + u\frac{\partial u}{\partial x} + v\frac{\partial u}{\partial y} + w\frac{\partial u}{\partial z}\right)\\
&\quad = \rho g_x + \frac{\partial}{\partial x}\tau_{11} + \frac{\partial}{\partial y}\tau_{12} + \frac{\partial}{\partial z}\tau_{13}\\
&\quad = -\frac{\partial p}{\partial x} + \rho g_x + B\frac{\partial}{\partial x}\left(\frac{\partial u}{\partial x}\right)^n + \frac{B}{2^n}\left[\frac{\partial}{\partial y}\left(\frac{\partial u}{\partial y} + \frac{\partial v}{\partial x}\right)^n + \frac{\partial}{\partial z}\left(\frac{\partial w}{\partial x} + \frac{\partial u}{\partial z}\right)^n\right]
\end{aligned}$$

which is the first equation of (2.2). The second and third equations of (2.2) are derived in a similar manner.

AUTHOR COPY

References

[1] F.D. Ellis, J.G. Seller III and C.W. Sewell, The second annular pulley: A histologic examination, *J. Hand Surg*. **20** (1995), 632–625.
[2] Y.C. Fung, *Biodynamics Circulation*, Springer-Verlag, New York, 1984.
[3] J.C. Guimberteau, J.P. Delage and J. Wong, The role and mechanical behavior of the connective tissue in tendon sliding, *Chirurgie de la main* **29** (2010), 155–166.
[4] A. Kandasamy and K.P. Vishwanath, Rheodynamic lubrication of a squeeze film bearing under sinusoidal squeeze motion, *Comp. Appl. Math*. **26** (2007), 381–396.
[5] B.M. Katzman, D.M. Klein, T.C. Garven, D.A. Caligiuri and J. Kung, Comparative histology of the annular and cruciform pulleys, *J. Hand Surg. Am*. **24** (1999), 272–274.
[6] D.M. Klein, B.M. Katzman, J.A. Mesa, J.F. Lipton and D.A. Caligiuri, Histology of the extensor retinaculum of the wrist and the ankle, *J. Hand Surg. Am.* **24** (1999), 799–802.
[7] T.C. Laurent and J.R. Fraser, Hyaluronan, *FASEB J*. **6** (1992), 2397–2404.
[8] D. McCombe, T. Brown, J. Slavin and W.A. Morrison, The histochemical structure of the deep fascia and its structural response to surgery, *J. Hand Surg. Br*. **26** (2001), 89–97.

[9] L.G. Nash, H. Nicholson, A.S.J. Lee, G.M. Johnson and M. Zhang, Configuration of the connective tissue in the posterior atlanto-occipital interspace: a sheet plastination and confocal microscopy study, *Spine* **30** (2005), 1359–1366.
[10] H. Ockendon and J. Ockendon, *Viscous Flow*, Cambridge Univ. Press, Cambridge, 1995.
[11] R. Panton, *Incompressible Flow*, 2nd edn, Wiley, New York, 1996.
[12] K. Piehl-Aulin, C. Laurent, A. Engstrom-Laurent, S. Hellstrom and J. Henriksson, Hyaluronan in human skeletal muscle of lower extremity: concentration, distribution, and effect of exercise, *J. Appl. Physiol*. **71** (1991), 2493–2498.
[13] M. Rivard, M. Laliberté, A. Bertrand-Grenier, C. Harnagea, C.P. Pfeffer, M. Vallières et al., The structural origin of second harmonic generation in fascia, *Biomed. Opt. Express* **2** (2010), 26–36.
[14] M. Roman, H. Chaudhry, B. Bukiet, C. Antonio and T. Findley, Flow of hyaluronan around fascia in rolfing, massage and fascial manipulation techniques: A comparative study, *JAOA* (2012), in press.
[15] J. Shukla, K. Prasad and P. Chandra, Effects of consistency variation of power law lubricants in squeeze films, *Wear* **76** (1982), 299–319.
[16] P. Sinha, J. Shukla, C. Singh and K. Prasad, Non-Newtonian lubrication theory for rough surfaces: Application to rigid and elastic rollers, *J. Mech. Eng. Sci*. **24** (1982), 147–154.
[17] C. Stecco, R. Stern, A. Porzionato, V. Macchi, S. Masiero, A. Stecco and R. De Caro, Hyaluronan within fascia in the etiology of myofascial pain, *Surg. Radiol. Anat*. **33** (2011), 891–896.
[18] R. Tadmor, N. Chen and J. Israelachvili, Thin film rheology and lubricity of hyaluronic acid solutions at a normal physiological concentration, *J. Biomed. Mater. Res.* **61** (2002), 514–523.
[19] G. Truskey, F.Yuan and D. Katz, *Transport Phenomena in Biological Systems*, 2nd edn, Pearson Prentice Hall, New Jersey, 2009.
[20] K.P. Vishvanathan and A. Kandaswamy, Rheodynamic lubrication of a rectangular squeeze film bearing with an exponential curvature variation using Bingham lubricants, *World Acad. Sci. Eng. Technol*. **43** (2008), 304–308.

AUTHOR COPY